

## INVESTIGATIONS OF PULSED LASER DEPOSITED TiN THIN FILMS FOR TITANIUM IMPLANTS

G. POPESCU-PELIN<sup>1,2</sup>, D. CRACIUN<sup>1</sup>, G. SOCOL<sup>1</sup>, D. CRISTEA<sup>3</sup>, L. FLOROIAN<sup>4</sup>, M. BADEA<sup>5</sup>,  
M. SOCOL<sup>6</sup>, V. CRACIUN<sup>1,\*</sup>

<sup>1</sup>National Institute for Lasers, Plasma and Radiation Physics, Magurele, Romania

<sup>2</sup>University of Bucharest, Faculty of Physics, Magurele, Romania

<sup>3</sup>Transilvania University, Materials Science Department, Brasov, Romania

<sup>4</sup>Transilvania University of Brasov, Faculty Elect Eng & Comp Sci., Romania

<sup>5</sup>Transilvania University of Brasov, Faculty of Medicine, Romania

<sup>6</sup>National Institute for Material Physics, Magurele, Romania

\*Corresponding author: valentin.craciun@inflpr.ro

Received October 16, 2015

*Abstract.* TiN thin films were deposited at room temperature on polished Ti samples by PLD. GIXRD investigations showed that films were crystalline, with grain sizes around 25 nm. Simulations of XRR curves indicated that the layers were dense and only slightly rougher than Ti substrates. Nanoindentation results showed that TiN films possessed a hardness of 26.8 GPa, much harder than Ti substrate, while scratch and wear tests found that films were adherent and exhibited a low friction coefficient of 0.16. Electrochemical tests performed in SBF indicated that the coated Ti samples exhibited significantly better behavior against corrosion than bare Ti samples.

*Key words:* pulsed laser deposition; thin films; TiN; mechanical properties; corrosion resistance.

### 1. INTRODUCTION

Biomaterials are nowadays widely used in the human body for various prostheses and orthopaedic devices [1]. Such biomaterials should be biocompatible, exhibit negligible dissolution rates in the body and have suitable mechanical properties for specific uses [2]. Ti and Ti-based alloys are widely used for metallic prosthesis and implants because they are biocompatible and possess many attractive chemical and mechanical properties [3, 4]. Unfortunately, Ti and its alloys also have several drawbacks. First, these materials have rather high friction coefficients resulting in substantial wear and tear during many years' time duration that the prosthesis are used [5]. Some of the crystallites could be dislodged from the prosthesis and cause an inflammatory reaction into the surrounding tissue [6]. It has been also shown that Ti has a low but still measurable dissolution rate in the body fluids [7, 8]. Since some prosthesis are quite big, possess a large area and

stay in the body for many years, the organs are exposed to a constant level of Ti ions that could accumulate in some parts and cause health problems [7, 9]. The combination between the poor mechanical properties and the slow dissolution rate limits the average life-time of prosthesis from 10 to max 25 years [10, 11]. Many patients will need to undergo a surgical revision during their life-time, which is both expensive and risky for older patients [11]. It is therefore critical to expand the life of prosthesis and implants, reduce the risks of inflammation and slow down the amount of released Ti ions into the body.

Since these problems are connected to the Ti surface the most effective way to avoid them is to coat the prosthesis and implants with biomaterials possessing better corrosion resistance, osseointegration, biocompatibility and reduced wear rates and debris amount and size [12–17].

One of the most used materials for protective coatings is TiN, which possess excellent physical and chemical properties, being also biocompatible [18–21]. Pulsed laser deposition (PLD) is an excellent technique to grow high quality films and investigate their properties once the droplet problem has been minimized [22]. We obtained high quality TiN films exhibiting very good mechanical properties using the PLD technique [23–25]. To decrease the grain size and avoid the oxidation of the Ti substrate we deposited TiN films at room temperature on pure Ti samples and investigated their mechanical and electrochemical properties in simulated body fluid (SBF). The structural, mechanical and electrochemical results are reported below.

## 2. EXPERIMENTAL DETAILS

Films were grown in a usual PLD experimental set up. A high purity TiN target was ablated by a KrF excimer laser ( $\lambda = 248$  nm, pulse duration  $\tau = 25$  ns,  $6$  J/cm<sup>2</sup> fluence, 40 Hz repetition rate, 40,000 pulses) under  $2 \times 10^{-3}$  Pa N<sub>2</sub> atmosphere [23–25]. The films were collected on (100) Si or mirror-like polished Ti substrates kept at room temperature. To study the films structure, grazing incidence and symmetrical X-ray diffraction (GIXRD and XRD) investigations were performed on the films with an Empyrean instrument (Panalytical) set to work in a parallel beam geometry with Cu  $K_{\alpha}$  radiation. The films mass density and surface roughness were obtained from simulations of the XRR curves, acquired with the same instrument, using a commercially available software (X'Pert Reflectivity). A model consisting of two layers, the deposited nitride or the Ti substrate and a thin surface contamination layer (SCL) accounting for the hydroxide/adventitious carbon layer present at the topmost surface when samples were exposed to the ambient was used for simulations. The surface topographic images were obtained by AFM with a Nanonics MultiView 4000 Microscope (intermittent contact mode) working in phase feedback. A tuning fork coated with

Cr having a 38 kHz resonance frequency and 1920 quality factor was used to scan ( $5 \times 5$ )  $\mu\text{m}^2$  area. Several scans were made on each sample in order to get an average value of root mean square (RMS).

The mechanical properties of the TiN thin film (hardness, elastic modulus) and of the titanium substrate were investigated using a nanoindentation device produced by CSM Instruments (NHT-2) equipped with a Berkovich diamond tip. To minimize substrate contributions, the indentation experiments were performed controlling the depth penetration of the indenter. The optimal penetration depth was determined after preliminary progressive multi-cycle mode (PMC) tests. This type of measurement allows for multiple indentations in the same spot on the sample, with increasing penetration depths/loads. The result is a series of hardness values, which, when plotted as a function of the penetration depth, gives an estimation of the optimal penetration depth for further fixed-depth nanoindentation measurements. The PMC measurements were performed with the following protocol: 25 cycles; the first penetration depth 10 nm; the last penetration depth 200 nm; loading rate 5 mN/min; unloading rate 50 mN/min. The fixed-depth nanoindentation measurements were performed with the same loading-unloading rates, and a penetration depth of 80 nm. The hardness and reduced modulus were determined following the model of Oliver and Pharr [18].

The adhesion of the TiN coating to the titanium substrates was determined using a Micro Scratch Tester (CSM Instruments) using a 100Cr6 steel tipped indenter with a Rockwell geometry (tip radius = 100  $\mu\text{m}$ ). The load was applied progressively with a speed of  $\sim 5$  N/min. The length of the tests was set at 3 mm. Dry wear tests were carried out at room temperature, using a ball-on-disk tribometer from CSM Instruments, in rotation mode. The variation of the dynamic friction coefficient against a 6 mm diameter sapphire ball (point-on-flat contact), was observed. Both the samples and the balls were ultrasonically cleaned in an ethanol bath prior to the wear tests. The normal load applied on the sapphire ball was 1 N. The stop condition was set at 20 m, in order to observe the friction coefficient variation as function of distance.

The behavior against corrosion of the bare and coated Ti samples was evaluated by sensitive electrochemical analyzes, in conditions which simulate the interaction with human body. The corrosion rate of the samples were determined by linear sweep voltammetry (LSV) in SBF using an Autolab PGSTAT100 Potentiostat (Eco Chemie), in a three electrodes configuration with a saturated calomel reference electrode (SCE) and a platinum wire as counter electrode. SBF has an ionic composition identical to blood plasma and was prepared by mixing the reagents, respecting the order and the quantities as indicated by Kokubo formula [27]. A batch of samples with 1  $\text{cm}^2$  active surface were immersed in SBF at 25° C and investigated after different immersion times. There is a linear relationship between the metal dissolution rate or corrosion rate, and the density of corrosion current  $i_{\text{corr}}$  that was calculated using Tafel Slope Analysis and Butler-Volmer

equation. Polarization Resistance,  $R_p$ , was also estimated and used to evaluate the resistance of the metal under investigation against corrosion. The LSV data were recorded with 0.008 V step potential, 0.04 V/s scan rate and the working potential was varied from  $-0.65$  V to  $+0.15$  V vs SCE.

### 3. RESULTS AND DISCUSSION

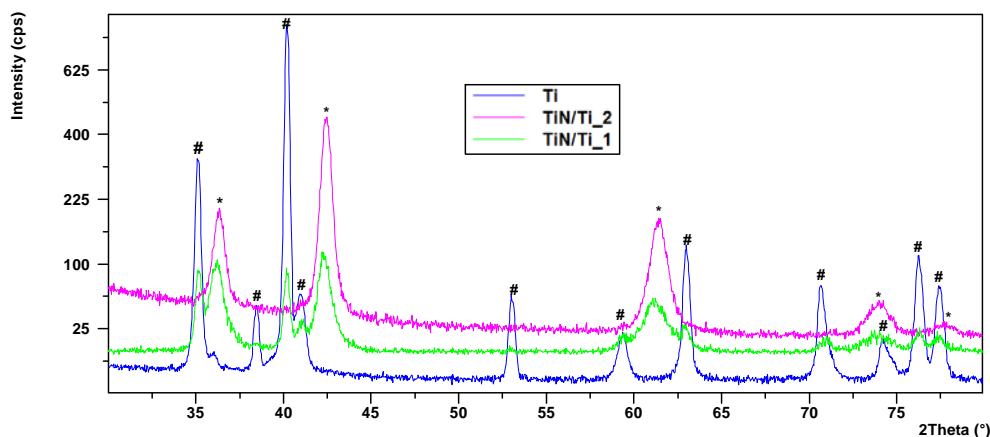


Fig. 1 – GIXRD patterns recorded from the bare Ti and TiN/Ti samples; for the TiN/Ti samples two incidence angles of  $2.0^\circ$  (green pattern) and  $0.2^\circ$  (pink pattern) were used.

Fig. 1 presents GIXRD patterns acquired from the bare Ti substrate and from TiN covered Ti samples, respectively. The diffraction peaks recorded from the bare Ti substrate (denoted by # in Fig. 1) were identified as belonging to  $\alpha$ -Ti (ICCD ref. pattern 98-004-3733, space group P 63/mmc,  $a = 2.9510$  Å,  $c = 4.6850$  Å) and a thin superficial  $\text{TiO}_2$  film that shares a very similar hexagonal lattice (ICCD ref. pattern 00-004-4872,  $a = 2.9190$  Å,  $c = 4.7130$  Å). For the TiN/Ti sample, besides the Ti peaks from the substrate, a cubic TiN having the lattice parameter  $a = 4.270$  Å (denoted by \* in Fig. 1, ICCD ref. pattern 00-065-8338, calculated density  $5.28$  g/cm<sup>3</sup>) was identified. For an incidence angle of  $0.2^\circ$ , only the TiN coating was observed, without any interference from the substrate. The grain size and microstress values estimated from Williamson Hall plots and line profile analysis (using the High Score Plus software) for these samples are also presented in Table 1. Results of the XRR curves simulations are shown in Table 1. The estimated density values are lower than the tabulated values, probably due to the roughness of the substrate, since the same films deposited on Si wafers showed densities values close to the tabulated one.

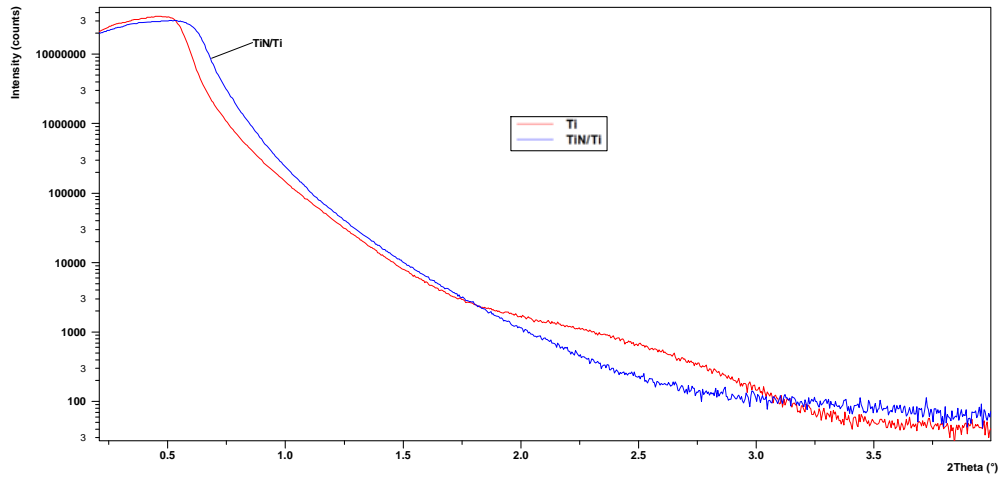


Fig. 2 – Comparison of XRR curves recorded from a bare Ti and TiN/Ti samples.

Table 1

XRR simulation results (SCL = surface contamination layer) and structural characteristics estimated from the Williamson-Hall plots and line profile analysis

Sample	Structure	Density (g/cm <sup>3</sup> )	Thickness (nm)	Roughness (nm)	Grain size WH/LPA [Å]	Micro-strain WH/LPA [%]
Ti	SCL	3.21	3.3	1.1	455/318	0.20/0.28
	Ti metal	3.84	NA	0.43		
TiN/Ti	SCL	2.19	1.06	0.94	52/25	0.90/0.59
	TiN	5.12	NA	2.2		

The AFM images recorded in the case of bare polished Ti substrate showed morphological features characterized by hollows and hills while the average RMS value was 4.1 nm (Fig. 3). Deposition of a thin TiN film on the surface of polished Ti slightly increased the RMS values to 7 nm. Moreover, the TiN film copies the substrate topography. In addition, random distributed spherical particulates with nanometric sizes (300–400 nm) were observed on the surface of films most likely generated during the laser ablation process [28].

Figure 4 presents the 25 loading-unloading curves from the PMC measurement (25 cycles) recorded from the TiN/Ti sample, as function of the penetration depth. Each hardness value from the PMC measurement was plotted as function of the penetration depth. If one analyzes the graph in Fig. 4, one can notice an increase in hardness up to a critical point, followed by a steady and significant decrease, towards, but not equal to representative values for the Ti substrate. The relatively low penetration depth and the hardening effect of the

remaining film are responsible for the difference between the hardness values (measured directly on the substrate and resultant from the PMC tests). For lower penetration depths ( $< 50$  nm), inconclusive hardness values could potentially be obtained as a consequence of the indentation size effect (ISE). The ISE is caused in general by the surface roughness, the presence of contamination layers on the sample surface or by indenter tip blunting, rather than by a true material effect [29]. Furthermore, considering that the measurements during the PMC test are done in the same spot, consecutive indentations would introduce tensions in the material, due to grain deformation, resulting in higher hardness values. Consequently, we concluded that an optimal penetration depth for the fixed-depth indentations would be in the 60–80 nm range, avoiding this way both the effects of the ISE and the tension-related hardening. The nanoindentation results for the TiN film and the titanium substrate, along with the critical loads observed after the adhesion tests, and the friction coefficient resultant from the wear tests, are presented in Table 2. The TiN film is significantly harder, compared to the titanium substrate.

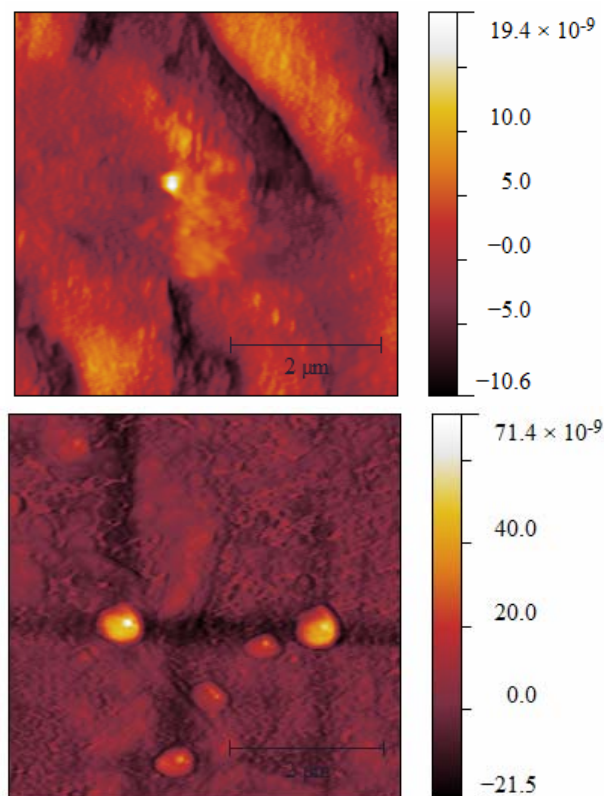


Fig. 3 – Typical AFM images of bare Ti substrate (RMS = 4.1 nm and Ra: 3.29 nm) and TiN/Ti sample (RMS = 7 nm and Ra: 4.55 nm).

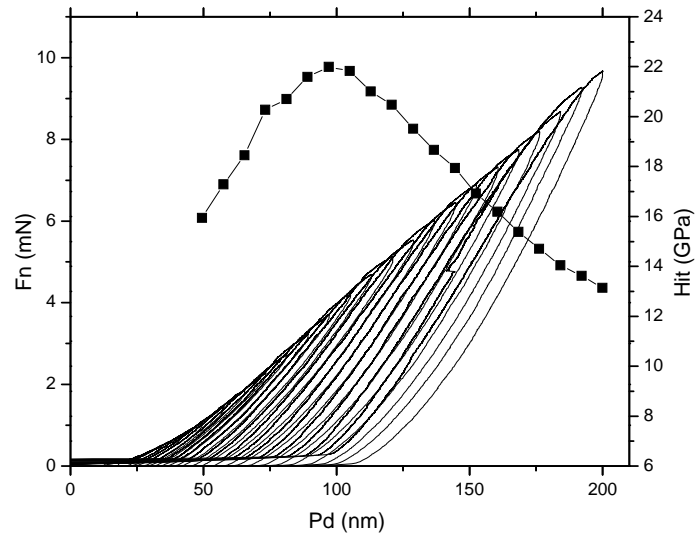


Fig. 4 – Progressive multi-cycle mode nanoindentation loading-unloading curves and hardness, both as function of the penetration depth, obtained from the TiN sample.

Table 2

Nanoindentation and adherence results for the TiN/Ti sample

Sample	Nanoindentation		Adherence			Friction coefficient
	Hit [GPa]	Eit [GPa]	Lc <sub>1</sub> [mN]	Lc <sub>2</sub> [mN]	Lc <sub>3</sub> [mN]	
TiN	26.81±1.92	236.81±19.18	–	404.12 ±80.09	1420.16 ±22.95	0.16
Ti (substrate)	2.66±0.18	157.94±6.39	–	–	–	0.49

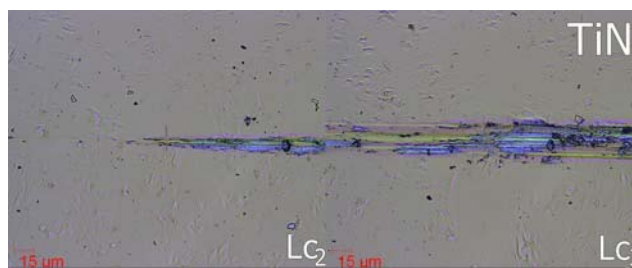


Fig. 5 – Film failure features, observed on the TiN coating deposited on titanium.

The adherence tests were confined to the samples' area of relatively uniform thickness. The critical load values were obtained after optical microscope analysis

of the wear tracks, and these are defined as follows:  $L_{c2}$  – the load necessary for the first film delamination (where the substrate is visible);  $L_{c3}$  – the load necessary for total film removal. Considering strictly the critical load values from Table 2, the TiN film is exhibiting a relatively average adhesion to the titanium substrate. This factor could be improved through several means: changing certain deposition parameters; using an intermediary layer as adhesion promoter; increasing the substrate roughness, etc.

The friction coefficient variation, as function of the distance, for the TiN coating and the bare Ti substrate, is presented in Fig. 6. One can notice a low friction regime for the entire test duration, in case of the TiN film, which would suggest that the film is wear resistant in these conditions, while the friction coefficient for the substrate, obtained in identical conditions, is significantly larger.

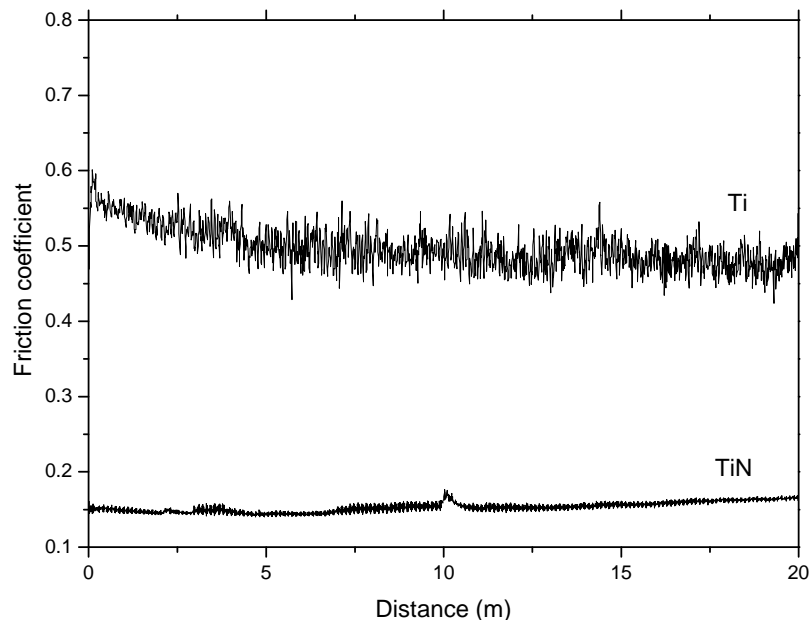


Fig. 6 – The variation of the friction coefficient as a function of the distance, for the TiN coating and the Ti substrate.

The degree of wear after 20 m can be observed in Fig. 7. The TiN coating was exhibiting a relatively low friction coefficient ( $\mu = 0.16$  – Table 2) and it was still present at the end of the test. This observation suggests that there is a clear correlation between the low friction coefficient and the good wear behavior of the TiN coating.

A material has a better resistance to corrosion if it has lower density of corrosion current, higher polarisation resistance and higher corrosion potential. All

these parameters for Ti and TiN/Ti samples were estimated by linear sweep voltammetry (LSV) analyses.

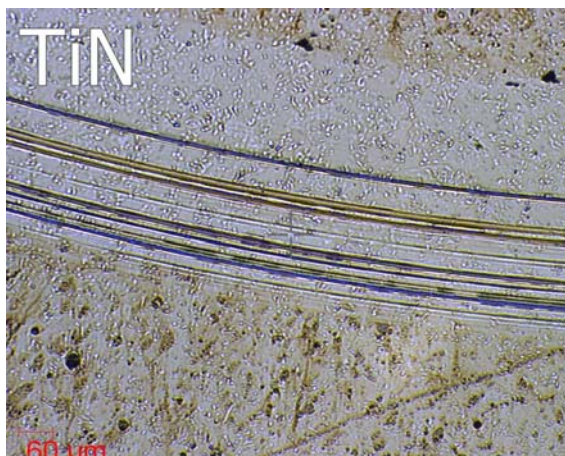


Fig. 7 – Wear track for the TiN coating obtained against a sapphire ball.

LSV results showed a good corrosion resistance for both types of initial samples, which exhibited similar values of corrosion parameters. After the initial evaluation, the samples of bare Ti and Ti covered with TiN thin films were introduced in SBF at room temperature and stored for 32 days. Afterwards, their Tafel spectra were recorded again and the corresponding corrosion parameters calculated (Table 3).

Table 3

Comparison between the initial corrosion parameters and those measured after 32 days of immersion in SBF

Sample	$i_{\text{corr}}$ ( $\mu\text{A}/\text{cm}^2$ )		$R_p$ ( $\text{k}\Omega$ )		$E_{\text{corr}}$ (mV)	
	initial	32 days	initial	32 days	initial	32 days
Ti	5.90	12.81	20.05	11.69	- 253	- 447
TiN/Ti	4.35	6.35	21.86	16.94	- 218	- 384

After 32 days of immersion in SBF, the density of the corrosion current of Ti sample reached a value significantly larger than that measured for TiN/Ti sample while its polarization resistance decreased almost twice. As it is known, an adherent, free of discontinuities Ti oxide film is formed on Ti surface when the surface is exposed to the ambient, which acts as a kinetic barrier preventing further oxidation and the loss of ions. When immersed in SBF the Ti passivation sharply

decreased and the density of corrosion current increased several orders of magnitude.

When Ti is immersed in SBF, chlorine ions are preferentially adsorbed on Ti oxide surface. The formed oxychloride compound is characterized by defects in the network and a greater solubility than the Ti oxide. So the chlorine ions promote ionization of the metal and the density of corrosion current increases as expected. For Ti samples covered with TiN thin films there are very small modifications of corrosion parameters implying a good behaviour against corrosion. A similar conclusion was reached after corrosion rate calculation; the bare Ti sample showed a 158  $\mu\text{m}/\text{year}$  corrosion rate, while by covering with TiN, the corrosion rate was reduced to 80  $\mu\text{m}/\text{year}$ , as displayed in Table 4.

Table 4

Corrosion rate of the samples after 32 days of immersion in SBF

Sample	Initial corrosion rate ( $\mu\text{m}/\text{year}$ )	Corrosion rate after 32 days ( $\mu\text{m}/\text{year}$ )
Ti	49.99	158.80
TiN/Ti	55.41	79.55

#### 4. CONCLUSION

TiN films were synthesized on polished Ti substrates using the pulsed laser deposition technique at room temperature. The TiN coatings were polycrystalline, dense and smooth.

Nanoindentation tests indicated a hardness of around 27 GPa, significantly higher than the corresponding value of 2.66 GPa measured for bare Ti samples. Scratch and wear tests showed a relatively good adhesion, a friction coefficient of 0.16 (compared to 0.49 for the Ti substrate) and low wear rates. The TiN/Ti samples were tested against corrosion in body simulated fluids for time durations up to 32 days. The results showed that the covering of titanium implants with TiN films is a good method to increase the corrosion resistance of Ti implants. The presence of the films on Ti surface considerably diminished implants' corrosion and the release of metallic ions into the solution.

**Acknowledgements.** This work was supported by grants of the Romanian Ministry of Education, CNCS – UEFISCDI, projects number IDEI 337/2012, STAR 65/2013 and PN-II-RU-PD-2012-3–0346.

This work was also supported by the Sectorial Operational Programme Human Resources Development (SOP HRD), financed from the European Social Fund and by the Romanian Government under the project number POSDRU/159/1.5/S/134378.

G. Popescu-Pelin gratefully acknowledges the Sectorial Operational Programme Human Resources Development (SOP HRD), financed from the European Social Fund and by the Romanian Government under the contract number SOP HRD/107/1.5/S/82514.

## REFERENCES

1. S. Bauer, P. Schmuki, K. von der Mark, J. Park, *Engineering biocompatible implant surfaces: Part I: Materials and surfaces*, Prog. Mat. Sci., **58**, 261–326 (2013).
2. C. Soundrapandian, S. Bharati, D. Basu, S. Datta, *Studies on novel bioactive glasses and bioactive glass–nano-HAp composites suitable for coating on metallic implants*, Ceram. Int., **37**, 3, 759–769 (2011).
3. C. Ohtsuki, H. Iida, S. Hayakawa and A. Osaka, *Bioactivity of titanium treated with hydrogen peroxide solutions containing metal chlorides*, J. Biomed. Mater. Res., **35**, 1, 39–47 (1997).
4. W. Wang and C. K. Poh, *Titanium Alloys in Orthopaedics*, J. Sieniawski and W. Ziaja eds., *Titanium Alloys – Advances in Properties Control*, InTech, Rijeka, Croatia, 1–20 (2013).
5. C. Met, L. Vandenbulcke, M.C. Sainte Catherine, *Friction and wear characteristics of various prosthetic materials sliding against smooth diamond-coated titanium alloy*, Wear **255**, 7–12, 1022–1029 (2003).
6. G. Longo, M. Girasole, G. Pompeo, A. Cricenti, C. Misiano, A. Acclavio, A.C. Tizzoni, L. Mazzola, P. Santini, L. Politi, R. Scandurra, *Effect of titanium carbide coating by ion plating plasma-assisted deposition on osteoblast response: A chemical, morphological and gene expression investigation*, Surf. Coat. Tech., **204**, 2605–2612 (2010).
7. H. Matusiewicz, *Potential release of in vivo trace metals from metallic medical implants in the human body: From ions to nanoparticles – A systematic analytical review*, Acta Biomaterialia **10**, 2379–2403 (2014).
8. N. Bruneel and J. A. Helsen, *In vitro simulation of biocompatibility of Ti-Al-V*, J. Biomed. Mater. Res., **22**, 3, 203–214 (1988).
9. M. Mohedano, E. Matykina, R. Arrabal, A. Pardo, M.C. Merino, *Metal release from ceramic coatings for dental implants*, Dent Mater., **30**, 3, e28–e40 (2014).
10. A. Holmberg, V. Gudrún Thórhallsdóttir, O. Robertsson, A. W-Dahl and A. Stefánsdóttir, *75% success rate after open debridement, exchange of tibial insert, and antibiotics in knee prosthetic joint infections*, Acta Orthop., **86**, 4, 457–462 (2015).
11. P. Mary, M. Bachy, É Mascarid, F. Gouin, *Secondary orthopaedic complications after childhood tumors of the musculoskeletal system*, Bull. Cancer, **102**, 7–8, 593–601 (2015).
12. E.M. Szesz, B.L. Pereira, N.K. Kuromoto, C.E.B. Marino, G.B. de Souza, P. Soares, *Electrochemical and morphological analysis on the titanium surface modified by shot blasting and anodic oxidation processes*, Thin Solid Films, **528**, 163–166 (2013).
13. C.E. Marino, S.R. Biaggio, R.C. Rocha-Filho, N. Bocchi, *Voltammetric stability of anodic films on the Ti6Al4V alloy in chloride medium*, Electrochim. Acta, **51**, 28, 6580–6583 (2006).
14. N. Diomidis, S. Mischler, N.S. More, M. Roy, S.N. Paul, *Fretting-corrosion behavior of beta titanium alloys in simulated synovial fluid*, Wear, **271**, 7–8, 1093–1102 (2011).
15. M P Licausi, A Igual Muñoz and V Amigó Borrás, *Tribocorrosion mechanisms of Ti6Al4V biomedical alloys in artificial saliva with different pHs*, J. Phys. D: Appl. Phys., **46**, 40, 404003 (2013).
16. V. Guiñón Pina, A. Dalmau, F. Devesa, V. Amigó, A. Igual Muñoz, *Tribocorrosion behavior of beta titanium biomedical alloys in phosphate buffer saline solution*, J. Mech. Behav. Biomed. Mater., **46**, 59–68 (2015).
17. A. Dalmau, V. Guiñón Pina, F. Devesa, V. Amigó, A. Igual Muñoz, *Electrochemical behavior of near-beta titanium biomedical alloys in phosphate buffer saline solution*, Mater. Sci. Eng. C Mater. Biol. Appl., **48**, 55–62 (2015).
18. V.S. Chathapuram, T. Du, K.B. Sundaram, V. Desai, *Role of oxidizer in the chemical mechanical planarization of the Ti/TiN barrier layer*, Microelectronic Eng., **65**, 4, 478–488 (2003).
19. I. Gotman, E. Y. Gutmanas, *Titanium nitride-based coatings on implantable medical devices*, Advanced Biomaterials and Devices in Medicine, **1**, 53–73 (2014).

20. S. Sedira, S. Achour, A. Avci, V. Eskizeybek, *Physical deposition of carbon doped titanium nitride film by DC magnetron sputtering for metallic implant coating use*, Appl. Surf. Sci., **295**, 81–85 (2014).
21. X. Shi, Lingli Xu, M.L. Munar, K. Ishikawa, *Hydrothermal treatment for TiN as abrasion resistant dental implant coating and its fibroblast response*, Mater. Sci. Eng. C Mater. Biol. Appl., **49**, 1–6 (2015).
22. V. Craciun, D. Craciun, M.C. Bunesco, C. Boulmer-Leborgne, J. Hermann, *Subsurface boiling during pulsed laser ablation of Ge*, Phys. Rev. B, **58**, 11, 6787–6790 (1998).
23. V. Craciun, D. Craciun, I. W. Boyd, *Reactive pulsed laser deposition of thin TiN films*, Mat. Sci. Eng. B-Solid State Mat. Adv. Technol., **18**, 178–180 (1993).
24. D. Craciun, N. Stefan, G. Socol, G. Dorcioman, E. McCumiskey, M. Hanna, C.R. Taylor, G. Bourne, E. Lambers, K. Siebein, V. Craciun, *Very hard TiN Thin Films Grown by Pulsed Laser Deposition*, Appl. Surf. Sci., **260**, 2–6 (2012).
25. D. Craciun, G. Socol, N. Stefan, G. Dorcioman, M. Hanna, C.R. Taylor, E. Lambers, V. Craciun, *The effect of deposition atmosphere on the chemical composition of TiN and ZrN thin films grown by pulsed laser deposition*, Appl. Surf. Sci., **302**, 124–128 (2014).
26. W.C. Oliver, G.M. Pharr, *An improved technique for determining hardness and elastic modulus using load and displacement sensing indentation experiments*, J. Mater. Res., **7**, 6, 1564–1583 (1992).
27. T. Kokubo, H. Kushitani, S. Sakka, T. Kitsugi, T. Yamamuro, *Solutions able to reproduce in vivo surface-structure changes in bioactive glass-ceramic A-W3*, J. Biomed. Mater. Res., **24**, 6, 721–734 (1990).
28. V. Craciun, N. Bassim, R.K. Singh, D. Craciun, J. Hermann, C. Boulmer-Leborgne, *Laser-induced explosive boiling during nanosecond laser ablation of silicon*, Appl. Surf. Sci., **186**, 1–4, 288–292 (2002).
29. T.F. Page, W.C. Oliver, C.J. McHargue, *The deformation behavior of ceramic crystals subjected to very low load (nano)indentations*, J. Mater. Res., **7**, 2, 450–473 (1992).